

Cyanine fluorophore derivatives with enhanced photostability

Roger B Altman¹, Daniel S Terry^{2,7}, Zhou Zhou^{1,7}, Qinsi Zheng³, Peter Geggier⁴, Rachel A Kolster⁴, Yongfang Zhao⁴, Jonathan A Javitch^{4,5}, J David Warren⁶ & Scott C Blanchard^{1-3,6}

Fluorescence applications requiring high photostability often depend on the use of solution additives to enhance fluorophore performance. Here we demonstrate that the direct or proximal conjugation of cyclooctatetraene (COT), 4-nitrobenzyl alcohol (NBA) or Trolox to the cyanine fluorophore Cy5 dramatically enhanced fluorophore photostability without otherwise affecting its native spectral characteristics. Such conjugation is a powerful means of improving the robustness of fluorescence-based applications demanding long-lived, nonblinking fluorescence emission.

Small organic fluorophores are powerful research tools in biological imaging that have enabled unprecedented insights into both cellular and molecular processes. However, their performance can be compromised by undesirable photophysical properties that limit both the fluorescence quantum yield and the total number of photons emitted before photobleaching. Such issues include both transient (blinking) and irreversible (photobleaching) light-induced transitions to dark states. Dark state transitions are particularly limiting in single-molecule studies that demand high illumination intensities. These problems are especially common to longer-wavelength fluorophores, such as Cy5, widely used in fluorescence resonance energy transfer-based investigations and applications demanding high signal-to-noise ratios.

The addition of small-molecule solution additives is a powerful means of minimizing fluorophore blinking and photobleaching both *in vitro* and *in vivo*¹⁻⁵. Common additives include triplet-state quenchers (TSQs) such as cyclooctatetraene (COT), 4-nitrobenzyl alcohol (NBA) and 6-hydroxy-2,5,7,8-tetramethylchroman-2-carboxylic acid (Trolox)^{2,3,6} that act in a concentration-dependent manner to reduce blinking rates, dark-state lifetimes and photobleaching rates².

Despite their advantages, TSQs have key limitations, including poor aqueous solubility, problems with membrane permeability and biological toxicity. To circumvent these issues, here we show that direct or proximal linkage of TSQs to the Cy5 fluorophore reduced blinking and photobleaching in both deoxygenated and oxygenated environments to extents exceeding those using TSQs in solution. We also observed enhanced Cy5 performance in living cells, suggesting these new fluorophore derivatives may be valuable for *in vivo* applications⁷.

In vitro single-molecule studies demonstrating that TSQs operate in a concentration-dependent fashion to affect the photophysical properties of cyanine fluorophores² suggest a collision-based mode of action⁸. To determine whether additional enhancements in fluorophore performance could be achieved by increasing the effective TSQ concentration beyond the solubility limit while simultaneously bypassing issues related to toxicity, we synthesized specific Cy5-TSQ conjugates in which we directly linked COT, NBA or Trolox to the fluorophore through a flexible, 12-atom linker (**Supplementary Fig. 1**). We developed a general strategy for the synthesis of such compounds by first modifying each TSQ to contain a single, amine-functional group followed by coupling it to the commercially available, bis-reactive, N-hydroxysuccinimidyl ester (NHS)₂-Cy5 fluorophore to yield a mono-functionalized NHS-Cy5-TSQ species at high efficiency (~30–60%) and purity (>98%) (**Fig. 1a** and **Supplementary Note**).

Bulk fluorescence measurements of the TSQ-conjugated Cy5 fluorophores demonstrated that absorption and emission spectra of TSQ-fluorophore conjugates were largely indistinguishable from those of the parent Cy5 compound, aside from modest shifts in fluorescence quantum yield (**Supplementary Fig. 2a,b**). The quantum yields for Cy5-COT, Cy5-NBA and Cy5-Trolox were increased by 25%, unchanged and decreased by 20%, respectively, compared to that for Cy5. Such changes may, in part, reflect variations in the apparent excited-state lifetimes (**Supplementary Fig. 2c**).

To evaluate these fluorophore derivatives, we reacted each compound with an amine- and biotin-functionalized, 21-base-pair, duplex DNA oligonucleotide that we purified to homogeneity using hydrophobic interaction chromatography (Online Methods). Using wide-field, total internal reflection fluorescence (TIRF) imaging², we assessed the photophysical properties of surface-immobilized fluorophore-DNA complexes at the single-molecule scale under direct laser illumination at 640 nm. We used typical single-molecule imaging conditions with an enzymatic oxygen-scavenging system to remove molecular oxygen from solution¹

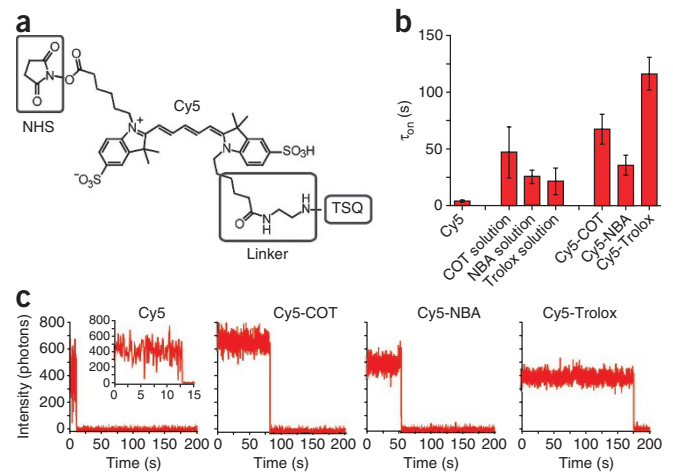
¹Department of Physiology and Biophysics, Weill Medical College of Cornell University, New York, New York, USA. ²Tri-Institutional Training Program in Computational Biology and Medicine, Weill Medical College of Cornell University, New York, New York, USA. ³Tri-Institutional Training Program in Chemical Biology, Weill Medical College of Cornell University, New York, New York, USA. ⁴Department of Psychiatry, Center for Molecular Recognition, College of Physicians and Surgeons, Columbia University, New York, New York, USA. ⁵Department of Pharmacology, College of Physicians and Surgeons, Columbia University, New York, New York, USA. ⁶Department of Biochemistry, Weill Medical College of Cornell University, New York, New York, USA. ⁷These authors contributed equally to this work. Correspondence should be addressed to S.C.B. (scb2005@med.cornell.edu).

Figure 1 | Enhancement of Cy5 photophysical properties through direct coupling to TSQs. **(a)** General schematic of TSQ-conjugated fluorophore derivatives. **(b)** Average dwell times in the on state (τ_{on}) with individual TSQs in solution (TSQ, solution) or directly conjugated to Cy5 (Cy5-TSQ). Error bars, s.d. ($n \geq 6$ movies from at least two independent experiments). **(c)** Representative traces of Cy5 fluorescence under direct excitation in the absence of TSQ (Cy5) and with COT, NBA or Trolox directly coupled to the dye.

and collected fluorescence trajectories for individual molecules. We analyzed the kinetic parameters of fluorescent and dark states using hidden Markov modeling. For simplicity, we focus here on the most salient fluorophore photophysical parameter, the average dwell time in the fluorescent ('on') state (τ_{on}).

At an illumination of 60 mW at the laser head and ~ 0.2 kW cm^{-2} at the image plane, the average τ_{on} of the parent Cy5 compound was ~ 4 s (**Fig. 1b**). Individual traces frequently exhibited brief periods of fluorescence punctuated by dark-state dwells characteristic of excursions to triplet states (**Fig. 1c**). In line with previous observations², the addition of 1 mM COT, NBA or Trolox to solution, approaching the solubility limit, increased τ_{on} by 5–12-fold (**Fig. 1b**).

Direct coupling of individual TSQ molecules to Cy5 substantially increased photostability compared to adding millimolar concentrations of TSQs in solution (**Fig. 1b,c** and **Supplementary Video 1**). In agreement with bulk measurements (**Supplementary Fig. 2**), mean fluorescence intensities of each of the Cy5-TSQ conjugates were similar to that of the parent Cy5 compound. Notably, however, the fluorescence intensity of Cy5-COT was higher ($\sim 60\%$) than that observed when imaging Cy5 (**Supplementary Fig. 3**). We observed similar trends over a range of illumination intensities and at a ten-fold higher time resolution (10 ms) (**Supplementary Figs. 4** and **5**). These enhancements are partially explained by the propensity of the parent Cy5 fluorophore to exhibit rapid blinking (**Supplementary Fig. 5a**). A calculation of μ , a parameter reflecting the number of photons emitted before photobleaching ($\tau_{on} \times$ average photon emission rate), indicated that the Cy5-TSQ conjugates tested are among the most photostable organic fluorophores available⁹ (**Supplementary Fig. 3b**). Each Cy5-TSQ conjugate also exhibited reduced rates of singlet-oxygen generation (**Supplementary Fig. 6**), suggesting that the performance



enhancements arise from a reduction in the frequency and/or duration of triplet-state excursions and a reduced likelihood of oxidative photodestruction.

To investigate whether direct coupling of TSQs to Cy5 was required for the enhancements observed, we affixed a single TSQ proximal to the fluorophore via linkage to residues in the DNA duplex. We synthesized NHS-reactive derivatives of COT, NBA and Trolox (**Supplementary Note**), and linked them to amine-modified thymine residues two base pairs distal to the site of fluorophore attachment (**Fig. 2a** and **Online Methods**). In each case, the proximal placement of a TSQ enhanced the performance of Cy5 (**Fig. 2b**). Although it was less effective than direct linkage, proximal linkage of the TSQ improved Cy5 performance comparably or better than 1 mM TSQ in solution (**Supplementary Fig. 7**). We examined the distance dependence of the protective effect by moving the Trolox molecule further away to positions 5 and 8 base pairs from the Cy5 attachment site and found that Cy5 enhancement correlated strongly with spatial proximity (**Fig. 2a,b**).

We used molecular dynamics simulations to obtain crude estimates of the spatial distributions of Cy5 and Trolox at their sites of attachment to the DNA oligonucleotide and their likelihood of collisional contact. In these analyses we considered the flexible nature of the Trolox and Cy5 attachment strategies (12-atom and 14-atom linkers, respectively), and found that frequent collisions between Cy5 and Trolox are only expected when Trolox is attached at positions 2 and 5 of the DNA duplex (**Fig. 2c**). Our findings support the collision-based mode of action

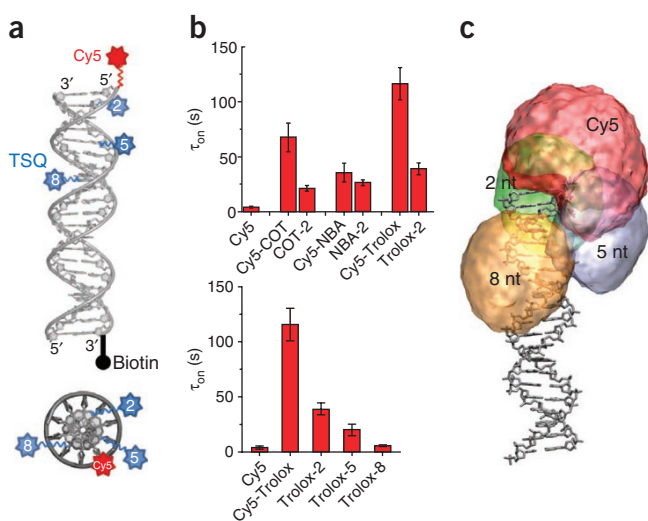


Figure 2 | Role of proximity in the enhancement of Cy5 fluorescence with indirectly coupled TSQs. **(a)** Schematic of the TSQ proximity experiment. DNA duplexes were created with one strand labeled with Cy5 (red) at the 5' end and TSQs (blue) 2, 5 and 8 nucleotides from the 3' end on the complementary strand. Views from the side (top) and above (bottom) are shown. **(b)** τ_{on} for constructs in which an individual TSQ was linked proximally to the Cy5 fluorophore 2 base pairs distal to the terminus of the DNA duplex (TSQ-2) (top). τ_{on} examined with Trolox attached at positions 2, 5 and 8 nucleotides away from the terminus of the DNA duplex (bottom). Error bars, s.d. ($n = 3$ movies). **(c)** Spatial distributions sampled by Cy5 and proximal TSQs determined using molecular dynamics simulations of DNA duplexes with Cy5 (red) labeled at the 5' end of one strand and one molecule of Trolox at one of three locations on the DNA helix: 2, 5 and 8 nucleotides (nt) from the 3' end of the complementary strand. Isosurfaces of the spatial distribution sampled by Cy5 and Trolox are shown as translucent clouds about the DNA helix.

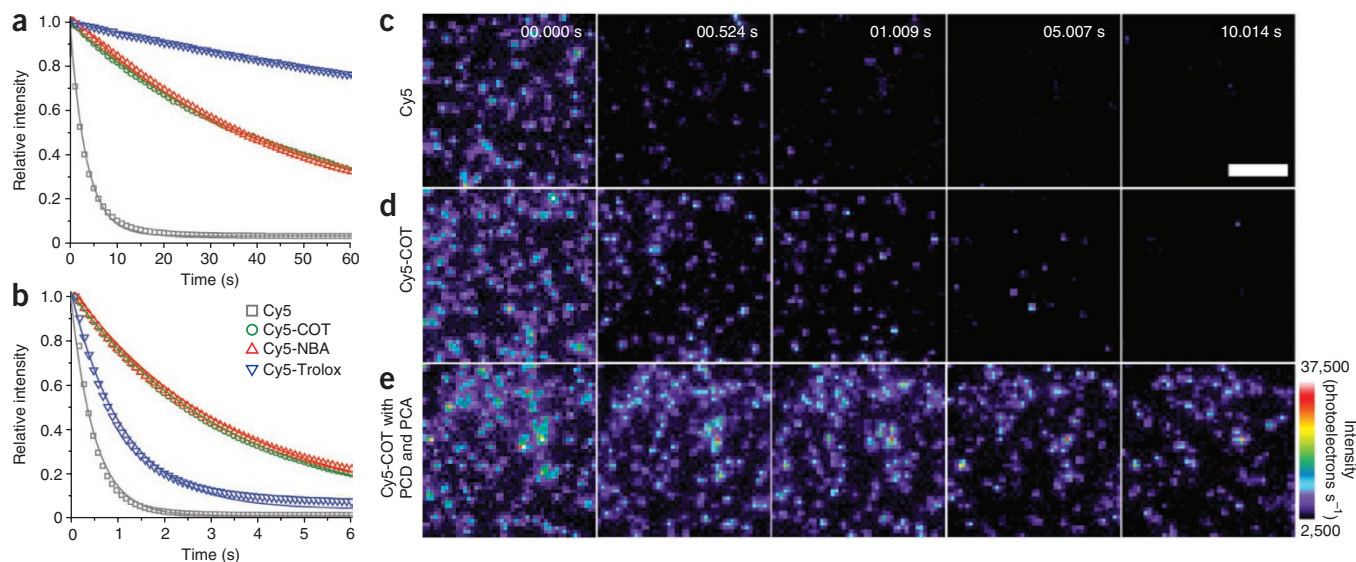


Figure 3 | Photostability of Cy5 and Cy5-TSQ conjugates in the presence of oxygen and in living cells. **(a,b)** Photostability of Cy5- and Cy5-TSQ-conjugated DNA duplexes surface-immobilized at a saturating density and in the presence **(a)** and absence **(b)** of an oxygen-scavenging system. Decay curves were fit to a single exponential process, and the time constants are reported in **Supplementary Table 1**. **(c-e)** Single-molecule total internal reflection fluorescence image sequences of living CHO cells containing dopamine D2 receptors labeled with Cy5 **(c)**, labeled with Cy5-COT **(d)** and labeled with Cy5-COT and imaged in deoxygenated solution containing 1 mM PCA and 50 nM PCD **(e)**. Scale bar, 5 μm .

and suggest that meaningful enhancements in fluorophore performance can be achieved by simply locating one or more TSQs in close physical proximity to the fluorophore.

To examine whether the improvements observed in Cy5 performance were particular to deoxygenated environments, we performed bulk and single-molecule photobleaching studies of immobilized molecules under both deoxygenated and oxygenated conditions. The benefits of direct conjugation of each TSQ to Cy5 were visually apparent (**Fig. 3a**). When >90% of the parent Cy5 fluorophore was photobleached, >80% of the Cy5 conjugates to TSQ remained active. In the absence of an oxygen scavenger, conditions more consistent with the cellular environment, we observed a substantial, albeit more modest (two- to sevenfold), reduction in photobleaching for each conjugate compared to the parent Cy5 compound (**Fig. 3b** and **Supplementary Table 1**). Single-molecule data indicated that each Cy5-TSQ conjugate exhibited stable fluorescence before photobleaching (**Supplementary Fig. 8**), suggesting that use of the conjugates may also enhance the sensitivity and signal-to-noise ratio in oxygenated environments. In contrast to the deoxygenated condition, Cy5-COT and Cy5-NBA performed better than Cy5-Trolox.

To investigate whether Cy5 conjugates to TSQ are effective at reducing photobleaching in a biological context under different experimental conditions, we performed single-molecule fluorescence imaging experiments on living Chinese hamster ovary (CHO) cells stably expressing an N-terminally SNAP-tagged, human dopamine D2 receptor¹⁰ labeled with either Cy5 or Cy5-COT (Online Methods). Consistent with the *in vitro* results, Cy5-COT label had a substantially improved τ_{on} compared to Cy5 (**Fig. 3c,d**). Introduction of oxygen-scavenging components (3,4-dihydroxybenzoic acid (PCA) and protocatechuic acid (PCD)) to the imaging solution dramatically enhanced this effect (**Fig. 3e**). In contrast, when we imaged Cy5-labeled D2 receptors under identical deoxygenated conditions,

reductions in photobleaching rate were accompanied by severe blinking, which reduced the signal-to-noise ratio and dramatically hampered the ability to image individual molecules (**Supplementary Video 2**). This improvement in fluorophore performance should allow robust single-molecule tracking over time scales relevant to signaling in the cellular context.

Technologies that enhance fluorophore stability are likely to be particularly advantageous for single-molecule fluorescence imaging where high illumination intensities are used to resolve fine signals over a range of timescales from milliseconds to minutes¹¹. Efforts must now be made to examine whether stability enhancements can be extended across the visual spectrum and to chemically distinct fluorophore species. Our fluorophore-TSQ conjugates may also be used for cellular investigations in which the use of solution TSQs may need to be avoided to preserve biological integrity or when imaging in the presence of oxygen is required. Both direct and proximal linkage strategies bypass problems of TSQ toxicity and solubility imposed by current techniques of adding one or more compounds to solution at high concentration. By increasing fluorophore stability and brightness, both methods also have the potential to improve the information content and signal-to-noise ratios in fluorescence imaging, allowing more robust tracking of processes over longer periods of time.

Our findings are consistent with a collision-based mechanism of action^{2,8}, where frequent, direct contact between the fluorophore and TSQ results in a net decrease in triplet-state occupancy and thus the rate of singlet-oxygen generation and photo-oxidation¹². The surprising finding, given the current literature^{5,13,14}, is that such effects can be achieved by a single TSQ, leaving open the possibility that combinations of different linked TSQs can mediate tailored enhancements in fluorophore performance. Such strategies may be particularly advantageous for multicolor fluorescence studies in which distinct fluorophores,

or the same fluorophore in unique environments, may respond preferentially, or negatively, to specific TSQ types². Efforts to test different fluorophore and TSQ combinations may also shed new light on the mechanism of TSQ action that will be useful for designing tailored compounds for distinct experimental demands.

METHODS

Methods and any associated references are available in the online version of the paper at <http://www.nature.com/naturemethods/>.

Note: Supplementary information is available on the Nature Methods website.

ACKNOWLEDGMENTS

This work was supported by the Tri-Institutional Training Program in Chemical Biology, the Tri-Institutional Training Program in Computational Biology and Medicine, the Irma T. Hirschl/Monique Weill-Caulier Trust and the Lieber Center for Schizophrenia Research and Treatment at Columbia University. We thank J. Paige, M. Feldman, M. Wasserman and L. Wang for critical feedback on the manuscript, and P. Whitford for help with and discussions about performing molecular dynamics simulations.

AUTHOR CONTRIBUTIONS

S.C.B., R.B.A. and D.S.T. designed *in vitro* experiments. Z.Z. and J.D.W. synthesized TSQ-conjugated fluorophores. R.B.A. made and purified complexes. R.B.A. performed single-molecule and bulk imaging experiments. Q.Z. performed bulk fluorescence and singlet-oxygen measurements. D.S.T. performed simulations. D.S.T., R.B.A. and S.C.B. analyzed *in vitro* data. S.C.B., J.A.J., and P.G. designed live-cell imaging experiments. Y.Z. and R.A.K. designed and constructed receptor constructs. P.G. performed the *in vivo* imaging and analyzed

data. R.B.A., D.S.T. and P.G. designed figures. R.B.A. and S.C.B. wrote the manuscript, which all authors edited.

COMPETING FINANCIAL INTERESTS

The authors declare no competing financial interests.

Published online at <http://www.nature.com/naturemethods/>.

Reprints and permissions information is available online at <http://www.nature.com/reprints/index.html>.

1. Aitken, C.E., Marshall, R.A. & Puglisi, J.D. *Biophys. J.* **94**, 1826–1835 (2008).
2. Dave, R., Terry, D.S., Munro, J.B. & Blanchard, S.C. *Biophys. J.* **96**, 2371–2381 (2009).
3. Rasnik, I., McKinney, S.A. & Ha, T. *Nat. Methods* **3**, 891–893 (2006).
4. Campos, L.A. *et al. Nat. Methods* **8**, 143–146 (2011).
5. Vogelsang, J. *et al. Angew. Chem. Int. Edn Engl.* **47**, 5465–5469 (2008).
6. Munro, J.B., Altman, R.B., O'Connor, N. & Blanchard, S.C. *Mol. Cell* **25**, 505–517 (2007).
7. Sakon, J.J. & Wening, K.R. *Nat. Methods* **7**, 203–205 (2010).
8. Marling, J.B., Gregg, D.W. & Wood, L. *Appl. Phys. Lett.* **17**, 527–530 (1970).
9. Roy, R., Hohng, S. & Ha, T. *Nat. Methods* **5**, 507–516 (2008).
10. Albizu, L. *et al. Nat. Chem. Biol.* **6**, 587–594 (2010).
11. Blanchard, S.C. *Curr. Opin. Struct. Biol.* **19**, 103–109 (2009).
12. Diaspro, A., Chirico, G., Usai, C. & Ramoino, P. in *Handbook of Biological Confocal Microscopy* (ed., Pawley, J.B.) 690–702 (Springer, 2006).
13. Cordes, T., Vogelsang, J. & Tinnefeld, P.O. *J. Am. Chem. Soc.* **131**, 5018–5019 (2009).
14. Vogelsang, J., Cordes, T., Forthmann, C., Steinhauer, C. & Tinnefeld, P. *Proc. Natl. Acad. Sci. USA* **106**, 8107–8112 (2009).

ONLINE METHODS

Generation of Cy5-TSQ-labeled DNA duplexes. A 21-nucleotide DNA, 5'-(5AmMC6)CATGACCATGACCATGACCAG(3BioTEG)-3', was chemically synthesized containing a 5' amino modifier with a six-carbon linker (5AmMC6) for fluorophore linkage and an additional 3' biotin moiety attached via a 22-atom tetra-ethyleneglycol (TEG) spacer (3BioTEG) (Integrated DNA Technologies). A complementary strand was synthesized with a C₆-amino thymine at various positions (indicated by asterisks) (5'-CTGGTCATGGTCAT*GGT*CAT*G-3').

Each DNA strand was individually labeled with either commercially available N-hydroxysuccinimide (NHS) ester activated fluorophore Cy5 (GE Healthcare) or newly generated TSQ-linked compounds (**Supplementary Note**) through the following procedure: lyophilized DNAs were resuspended in double-distilled (dd)H₂O and adjusted to 50 μM in 50 mM potassium borate buffer (pH 8.1) with 200 mM KCl. Labeling was achieved by adding a five-fold molar excess of NHS-reactive fluorophore or TSQ resuspended in dimethyl sulfoxide (DMSO) in a 10-μl reaction. After incubation at 37 °C for 30 min, all reactions were quenched with 0.2 μl of 1 M Tris-acetate pH 7.5 at 25 °C for 2 min. Complementary strands were hybridized by mixing the two in equimolar ratios, briefly heating to 90 °C followed by passive cooling to room temperature (23 °C). Unbound fluorophore was removed using 300 μl of diethylaminoethyl (DEAE) cellulose resin equilibrated with 10 mM Tris-acetate (pH 7) with 200 mM ammonium chloride. Hybrids were diluted in column buffer for binding, then after extensive washing to liberate free fluorophore, the DNA was eluted with 10 mM Tris-acetate (pH 7) with 1 M ammonium chloride. Labeled fractions were pooled (~200 μl total), diluted in 1 ml of buffer A (1.7 M ammonium sulfate, 10 mM ammonium acetate pH 5.85) and applied over an (FPLC) phenyl 5PW column (Tosoh Bioscience) using a 60-min gradient from buffer A to B (10% methanol and 10 mM ammonium acetate; pH 5.85). The major peak of interest was collected and used for single-molecule experiments.

Bulk absorption spectra measurements were performed using a 1240 mini UV-VIS spectrophotometer (Shimadzu). Bulk emission spectra measurements were performed using a PTI spectrofluorometer with excitation at 629 nm, normalized by the absorption. Quantum yields were calculated as the area under these emission curves. Fluorescence lifetime measurements were conducted using a PTI fluorescence lifetime system, with 0.5% milk in water as a blank. Double-exponential fitting was performed and the fluorescence lifetime was estimated by the weighted average of the fitting. For the experiments described **Supplementary Figure 2**, dyes were dissolved in methanol and measurements were taken in a 10-mm-pathlength cuvette.

Single-molecule imaging of Cy5-TSQ-labeled DNA duplexes.

All experiments were performed using a laboratory built, prism-based total internal reflection fluorescence (TIRF) apparatus as previously described² at specified illumination intensities in T50 buffer (10 mM Tris acetate (pH 7.5) and 50 mM KCl), containing 5 mM β-mercaptoethanol, 1 mM 3,4-dihydroxybenzoic acid (PCA) and 50 nM protocatechuate 3,4-deoxygenase (PCD) (Sigma-Aldrich). Biotinylated DNA molecules were immobilized via a biotin-streptavidin interaction in microfluidic channels constructed on quartz slides^{2,6}. Fluorescence from surface-immobilized

molecules, illuminated via the evanescent wave generated by total internal reflection of a 640 nm (Coherent) laser source, was collected using a 1.27 numerical aperture (NA), 60× water-immersion objective (Nikon) and imaged onto a Cascade Evolve 512 electron-multiplying charge-coupled device (EMCCD) camera (Photometrics). Data were acquired using Metamorph software (Universal Imaging Corporation) collecting at a frame rate of 10–100 s⁻¹. Bulk studies were performed by immobilizing a saturating amount of molecules under deoxygenated and oxygenated conditions. Fluorescence decay curves (**Fig. 3a,b**) were created by averaging intensity over the field of view for each frame and fitting to single-exponential distributions.

Kinetic analysis of fluorescence time traces. The photophysical properties of fluorophores were investigated using automated software built in-house using MATLAB (MathWorks) as previously described². Traces were extracted from wide-field TIRF movies by finding peaks of fluorescence intensity at least 8 s.d. above background noise and summing the intensity of 4 total pixels encompassing each peak. Neighboring peaks closer than 2.1 pixels were removed.

To reduce analytical error, traces were only used for analysis if they passed the following criteria: signal-background noise ratio >10, single-step photobleaching and background noise levels within 4 s.d. from the mean.

To extract kinetic parameters of blinking and photobleaching, the fluorescence traces were normalized to the mean fluorescence intensity of each dataset and idealized using the segmental K-means (SKM) algorithm¹⁵ and a three-state model with one fluorescent (on) state, a transient dark state (blinking) and a permanent dark state (photobleaching). τ_{on} was calculated by fitting the cumulative distribution (survival plot) to an exponential function. Total τ_{on} was calculated by taking the mean of the distributions of the total time spent in the on state in each trace. Photon counts were calculated from analog-to-digital units using a conversion provided by the manufacturer.

Measurement of singlet oxygen. Singlet oxygen generation rates were measured using diaminobenzide (DAB) as a reporter. Upon oxidation by singlet oxygen, the insoluble oxidized products of DAB could be measured in solution as an increase in optical density (OD) from 350 nm to 650 nm¹⁶. Assayed solution contained 133 μM DAB, 8 μM dye (Cy5 or Cy5-TSQ), 5 mM β-mercaptoethanol and 2 mM PCA in T50 buffer. As a control experiment, PCD was also added (8 nM final concentration) into the solution to remove oxygen. Reactions were run in a 100-μl, 10-mm-pathlength cuvette, illuminated using a 75 mW, 640 nm laser. Absorbance at 400 nm was measured before the illumination and after 2, 4, 8, 12, 16 and 20 min of illumination, in a 1240 mini UV-VIS spectrophotometer (Shimadzu). The starting optical density was adjusted to 0 and linear fitting was performed with a fixed y-intercept at 0. The relative rate of singlet oxygen generation for Cy5 and Cy5-TSQ dyes was estimated by the slope of the increase in optical density.

Molecular dynamics simulations. Molecular dynamics simulations of fluorophore-labeled DNA duplexes were performed to estimate the average distance between the Cy5 fluorophore and proximal DNA-linked TSQs. DNA duplex models were

constructed with nucgen¹⁷. Fluorophore molecules were constructed and geometry optimized in Avogadro and attached to modified thymine residues in the structure at specific locations: Cy5 at the 5' end of one strand and a Trolox molecule at internal positions on the complementary strand: 2, 5 and 8 nucleotides from the 3' end. Simulations were performed using a structure-based potential¹⁸ with Groningen machine for chemical simulations (GROMACS)¹⁷, where only contacts in the DNA duplex have attractive Van der Waals interactions to maintain the structure. This simple potential allows the fluorophore and TSQ to freely diffuse and rotate according to the constraints of the linker and DNA duplex, but requires less computational power than with a full empirical force field.

Simulations were run for 100 ns (10^8 time steps) each. The space sampled by Cy5 and TSQs was calculated using the VolMap Tool in visual molecular dynamics (VMD)¹⁹. For Cy5, all atoms in the headgroup were included.

Cell culture and media. Flp-in Chinese hamster ovary (CHO) cells (Invitrogen) were stably transfected with pcDNA6/TR (Invitrogen), and single clones were selected with $15 \mu\text{g ml}^{-1}$ blasticidin and $100 \mu\text{g ml}^{-1}$ zeocin. The clone with the lowest basal expression and highest induction ratio in response to overnight treatment with $1 \mu\text{g ml}^{-1}$ tetracycline was stably transfected with a pcDNA5/FRT/To-IRES construct encoding the human dopamine D2 receptor short isoform (D2s) with a SNAP tag (NEB) fused to its N terminus, and single clones were selected in $200 \mu\text{g ml}^{-1}$ hygromycin in the continued presence of $15 \mu\text{g ml}^{-1}$ blasticidin. To reduce receptor expression for ease of single-molecule tracking, the Kozak sequence was mutated to thymine at the -3 and +4 position sites, and the CMV enhancer sequence was partly deleted by digestion with NruI and SnaBI (from position 209 to 591) and religation. Cells were maintained in Ham's F-12 medium (Cellgro) containing 10% FBS and 1% glutamine at 37 °C in 5% CO₂, in the presence of blasticidin ($15 \mu\text{g ml}^{-1}$) and hygromycin ($200 \mu\text{g ml}^{-1}$). Cells were used without tetracycline induction to limit receptor expression.

Cell labeling and preparation for TIRF imaging. When cells reached ~70% confluence, they were washed with PBS, resuspended in enzyme-free cell dissociation buffer (Millipore) and incubated in suspension with 10 nM BG-Cy5 or BG-Cy5-COT (in 0.1% (vol/vol) DMSO and PBS) for 1 h at 37 °C. BG-derivatives of Cy5 and Cy5-COT were prepared by standard procedures in which O6-(4-(aminomethyl)benzyl)guanine (BG) was linked to NHS-derivatives of Cy5 and Cy5-COT, respectively, followed by high-performance liquid chromatography (HPLC) purification. This concentration was chosen based on fluorescence-activated cells

sorting (FACS) analysis to label only ~5% of the surface receptors to facilitate particle tracking. Cells were then washed twice with 0.1% DMSO and Dulbecco's phosphate-buffered saline (DPBS) (Cellgro) and once with 0.1% BSA and DPBS. Cells were seeded on fibronectin-coated ($0.1 \mu\text{g } \mu\text{l}^{-1}$) (Sigma-Aldrich), 25 mm, #1.5 glass coverslips (Warner Instruments) and incubated in phenol-red-free DMEM/F12 medium (Gibco) containing 10% FBS and 1% glutamine for at least 1 h. Before use, new coverslips were cleaned with an optical lens cleaner (Sparkle; A.J. Funk and Co.), followed by incubation for 1.5 h in a 1:0.25:5 solution of hydrogen peroxide and ammonium hydroxide in deionized water at 75 °C. Coverslips were subsequently rinsed in deionized water, then rinsed in 100% ethanol, rapidly dried with filtered air and passed several times over a flame. Before imaging, the coverslip with cells attached was washed seven times in PBS, the coverslip was assembled into an imaging chamber (RC-40LP, Warner Instruments) and the chamber was filled with Hank's balanced salt solution (HBSS) (Gibco) (1.26 mM calcium chloride, 0.493 mM magnesium chloride, 0.407 mM magnesium sulfate, 5.33 mM potassium chloride, 0.441 mM potassium phosphate monobasic, 4.17 mM sodium bicarbonate, 137.93 mM sodium chloride, 0.338 mM sodium phosphate dibasic and 5.56 mM D-glucose). Immediately before imaging, PCA and PCD were diluted in HBSS to reach a final concentration of 1 mM and 50 nM, respectively, in the imaging chamber.

Microscopy. Image sequences of single D2 receptors were measured using an objective-based TIRF microscope (IX81 with CellTIRF illuminator, Olympus) equipped with a 100× oil-immersion objective (100xUAPON NA 1.49, Olympus). Focus drift during data acquisition was minimized by using a laser autofocus system (ZDC2, Olympus) in continuous focusing mode. To establish evanescent wave illumination of receptor labeled BG-Cy5 derivatives, the excitation light beam of a red laser (640 nm, 100 mW, Olympus) was focused into the back focal plane of the objective at an angle of incidence of 76.21°, resulting in an approximate penetration depth of 90 nm. The average laser intensity during each measurement at the specimen plane was $\sim 0.5 \text{ kW cm}^{-2}$. Fluorescence emission was separated from excitation light using a full-multiband filter set (LF405/488/561/635, Semrock) in combination with a single-bandpass filter (FF01-685/40, Semrock) and recorded with an EMCCD camera (Evolve 512, Photometrics) at a time resolution of 40 ms.

15. Qin, F. *Biophys. J.* **86**, 1488–1501 (2004).

16. Deerinck, T.J. *J. Cell Biol.* **126**, 901–910 (1994).

17. Hess, B. *J. Chem. Theory Comput.* **4**, 435–447 (2008).

18. Whitford, P.C. *et al. Proteins* **75**, 430–441 (2008).

19. Humphrey, W., Dalke, A. & Schulten, K. *J. Mol. Graph.* **14**, 33–38 (1996).